Effect of fluorination on preparation of Bi(Pb)SCCO 2 2 2 3 by the citrate precursor process

J. H. GREENBERG, L. BEN-DOR
Department of Inorganic and Analytical Chemistry, Hebrew University, 91904 Jerusalem, Israel

V. BEILIN
School of Applied Science and Technology, Hebrew University, 91904 Jerusalem, Israel

D. SZAFRANEK
EPMA Lab, Institute of Earth Sciences, Hebrew University, 91904 Jerusalem, Israel

Citrate precursor technology was used to prepare fluorine substituted Bi(Pb)SCCO 2 2 2 3 superconducting phase. Samples with the nominal composition of up to three F atoms per formula were synthesized. A number of experimental methods have been used to characterize the samples and to trace the phase transformations during the preparation process: DTA/TGA, XRD, EPMA (WDS and EDS), atomic absorption, potentiometry with fluoride selective electrode, resistance and inductive measurements. Fluorine was shown to enhance considerably the formation of the 2 2 2 3 phase. Thermodynamic calculations of P–T–X equilibrium in the Bi–Pb–Sr–Ca–Cu–O–F–C–H–N system were made in a wide temperature range to determine the composition of the vapours coexisting with the solid phases at different stages of the preparation process.

1. Introduction

Ever since the discovery of high temperature superconductivity (HTSC) in oxides, great effort has been invested in preparation of substituted derivatives. The majority of publications deals with cation doping, although anion substitution was also reported. In particular, attempts have been made to introduce fluorine into different types of HTSC: La_2CuO_4 [1,2], YBCO [3,4], BSCCO [5–11]. Fluorine substituted BSCCO has been prepared mainly by solid state reactions with or without subsequent vapour phase treatment. Only in one publication (Kemnitz *et al.* [11]) was a different technique (freeze drying) applied for that purpose.

In this paper we report the first study of fluorine substitution in BSCCO 2 2 2 3 via citrate technology and the influence of fluorine on this process.

2. Pressure–Temperature–Composition (P–T–X phase) equilibrium

Prior to experimental research, calculations of phase equilibria in the Bi–Pb–Sr–Ca–Cu–O system were made, since up till now only condensed phase equilibria in this system were studied and no data on composition of the vapours is available. Meanwhile, this information is crucial for preparation of the material because of partial sublimation of different species during the preparation procedure and incongruent sublimation of the material itself. Recent extensive research

in the thermochemistry of mixed oxides in this system [12,13] made it possible to calculate the equilibrium composition in a wide P–T–X range and simulate different preparation routes for HTSC. For this purpose the thermodynamic database Ivtantermo [14] was used and temperature dependences of heat capacities of mixed oxides were adjusted according to the temperature limits of stability of complex oxides on the T–X projection of the phase diagram Bi_2O_3–PbO–SrO–CaO–CuO as compiled by Majewski [15]. The calculation procedure has been described in detail by Sinyarev and co-workers [16]. The equilibrium composition was calculated at pressures up to 1.013×10^6 Pa and temperatures up to 1500 K in oxygen, air, inert atmosphere (argon) and vacuum. A total of 43 individual condensed phases and 135 vapour species were taken into account in this treatment. Phase equilibria in Bi–Sr–Ca–Cu–O were studied as well as doping of Bi–HTSC materials. As it turned out, the P–T–X region of the single phase existence of BSCCO 2 2 1 2 was due to the entropy stabilization of this compound in respect to other mixed oxides in the Bi_2O_3–SrO–CaO–CuO system. A similar result was obtained from the high temperature heat capacity measurements of YBCO-123 which showed that this compound was entropy-stabilized in the Y_2O_3–BaO–CuO system with regard to other complex oxides [17].

Table I lists the composition of the vapours in 1.013×10^5 Pa air in equilibrium with the condensed

TABLE I Composition of the vapours (Pa) in air at 1.013×10^5 Pa

	Temperature (K)						
	1173	1123	1073	1023	973	923	873
O	6.28×10^{-4}	1.92×10^{-4}	5.57×10^{-5}	1.41×10^{-5}	3.0×10^{-6}	5.57×10^{-7}	8.51×10^{-8}
O_2	1.92×10^4	1.92×10^4	1.92×10^4	1.92×10^4	1.92×10^4	1.92×10^4	1.92×10^4
OH	5.87×10^{-2}	2.83×10^{-2}	1.21×10^{-2}	5.06×10^{-3}	1.92×10^{-3}	6.48×10^{-4}	1.92×10^{-4}
HO_2	3.54×10^{-4}	2.02×10^{-4}	1.01×10^{-4}	5.06×10^{-5}	2.32×10^{-5}	9.72×10^{-6}	3.64×10^{-6}
H_2O	8.30×10^2	8.30×10^2	8.30×10^2	8.30×10^2	8.30×10^2	8.30×10^2	8.30×10^2
HF	0.67×10^1	0.39×10^1	0.25×10^1	0.14×10^1	9.21×10^{-1}	4.55×10^{-1}	2.02×10^{-1}
N_2	8.00×10^4	8.00×10^4	8.00×10^4	8.00×10^4	8.00×10^4	8.00×10^4	8.00×10^4
NO	1.51×10^1	1.01×10^1	0.63×10^1	0.38×10^1	0.22×10^1	0.12×10^1	6.17×10^{-1}
NO_2	2.93×10^{-1}	2.43×10^{-1}	2.02×10^{-1}	1.72×10^{-1}	1.41×10^{-1}	1.11×10^{-1}	8.71×10^{-2}
N_2O	1.11×10^{-3}	7.39×10^{-4}	4.86×10^{-4}	3.14×10^{-4}	1.92×10^{-4}	1.11×10^{-4}	5.87×10^{-5}
HNO_2	5.87×10^{-4}	4.86×10^{-4}	3.84×10^{-4}	3.03×10^{-4}	2.32×10^{-4}	1.72×10^{-4}	1.21×10^{-4}
CO_2	9.52×10^2	9.52×10^2	9.52×10^2	9.52×10^2	9.11×10^2	9.11×10^2	9.11×10^2
Pb	2.32×10^{-3}	3.54×10^{-4}	6.17×10^{-5}	6.78×10^{-6}	5.97×10^{-7}	4.05×10^{-8}	1.92×10^{-9}
PbO	0.42×10^1	0.12×10^1	3.84×10^{-1}	8.61×10^{-2}	1.62×10^{-2}	2.63×10^{-3}	3.24×10^{-4}
PbO_2	8.91×10^{-2}	3.14×10^{-2}	1.41×10^{-2}	4.15×10^{-3}	1.11×10^{-3}	2.63×10^{-4}	5.06×10^{-5}
Pb_2O_2	0.82×10^1	0.21×10^1	7.69×10^{-1}	1.62×10^{-1}	2.7×10^{-2}	3.95×10^{-3}	4.35×10^{-4}
PbF	1.21×10^{-4}	1.92×10^{-5}	3.74×10^{-6}	4.35×10^{-7}	5.16×10^{-8}	3.74×10^{-9}	2.02×10^{-10}
PbF_2	1.51×10^{-3}	3.54×10^{-4}	1.21×10^{-4}	2.43×10^{-5}	6.48×10^{-6}	9.01×10^{-7}	9.92×10^{-8}
SrF_2	1.31×10^{-4}	2.02×10^{-5}	2.73×10^{-6}	3.03×10^{-7}	2.93×10^{-8}	7.39×10^{-10}	1.21×10^{-11}
CuF	1.62×10^{-4}	2.63×10^{-5}	3.95×10^{-6}	4.65×10^{-7}	5.36×10^{-8}	1.46×10^{-9}	1.92×10^{-10}

phases during the sol–gel preparation of the 2 2 2 3 compound doped with lead and fluorine. The initial composition is a mixture of $Bi_{1.65}Pb_{0.35}Sr_2Ca_2Cu_3O_{10}F_{0.7}$, citric acid and ethylene glycol. From these results it should be anticipated that a considerable loss of fluorine in the form of HF is to be expected in an open system in the preliminary stages of the preparation when the partial pressure of HF is 0.1013–1.013 Pa. During sintering a certain portion of lead can be lost due to vaporization of lead oxides (partial pressures of PbO and Pb_2O_2 at 1073–1123 K are 0.1013–1.013 Pa). On the other hand, no appreciable loss of fluorine should be expected at the sintering stages, since the partial pressures of the metal fluorides are quite low $(1.013 \times 10^{-6} – 1.013 \times 10^{-4}$ Pa).

A point to be stressed here is that, according to this P–T–X study, the upper temperature limit of stability of the 2 2 2 3 phase depends on the sintering environment; in an inert gas (argon) it is about 1073 K which is 50 K lower than in air (1123 K).

3. Experimental details
3.1. Preparation
Sol–gel citrate technology was applied since this method has been successfully used in this laboratory and elsewhere for preparation of single phase and homogeneous undoped 2 2 2 3 compound [18–20]. The starting materials were the corresponding nitrates and PbF_2 (or PbF_2 + CuF_2) with the initial fluorine concentrations up to three atoms per formula. The mixture of salts was dissolved in nitric acid (1:20). Citric acid and ethylene glycol were added to the solution at the molar ratio 2:1 (2 mol both of citric acid and ethylene glycol to 1 mol of the sum of the cations). The mixture was heated on a hot plate with a magnetic stirrer at 353 K for about 1 h, until a blue viscous gel was formed. Afterwards it was pyrolysed

at 473 K. At this stage spontaneous combustion of organics was observed and brown-to-black flakes of a fine particle material was formed. This residue was pulverized and calcined at 773 K for 3 h, then reground and calcined for a further 3 h at 1073 K to ensure elimination of the organic components. The resulting powder was pelletized with a load of 10.16 tonne at room temperature and sintered at 1113 K to 1133 K for 24–210 h with intermediate regrinding and repelletizing.

3.2. Characterization
The samples were characterized by X-ray diffraction (XRD), differential thermal analysis/thermogravimetric analysis (DTA/TGA), and electron probe X-ray microanalysis (EPMA). The cations were analysed by atomic absorption (Perkin–Elmer 403 atomic absorption spectrophotometer), and the fluorine concentration was measured by means of potentiometry with a standard fluoride selective electrode. Superconductive transition was characterized by the resistance measurements and an inductive method [21,22]. X-ray diffraction patterns were recorded on a Philips X-Ray powder diffractometer with CuK_α radiation. Simultaneous DTA and TGA were used both to characterize the samples after the complete preparation cycle and for following the mechanism of phase transformations during the different stages of preparation. For this purpose a Stanton–Redcroft model STA-781 instrument was used. The samples (25–45 mg) were contained in inconel microcrucibles, while the reference was calcined alumina powder. The measurements were made at a heating rate of 10 K min^{-1} from room temperature up to 1223 K under flowing argon gas. The apparatus was calibrated against melting temperatures of the usual standards: Zn (692.7 K), Sb (903.5 K), NaCl (1074 K), Ag

(1235 K), which spanned the whole temperature range of the investigation. For EPMA a Jeol JXA–8600 electron microanalyser was used equipped with four wave dispersive spectroscopy (WDS) spectrometers and an energy dispersive spectroscopy (EDS) analytical system from Tracor Northern. Most of the observations were made with a 15 KeV, 10 nA electron beam. Back scatter electron mode was used to discern different phases. Quantitative analysis was performed by combined WDS–EDS spectrometry. Strontium was calibrated against $SrCO_3$, calcium against $CaCO_3$, copper against Cu_2O, bismuth and lead against the metals, and fluorine against CaF_2. Reproducible results could not be obtained on an untreated surface of the pellets; therefore the pellets were polished. A standard polishing technique with ethanol–water solution for washing and lubrication led to a certain interaction with the sample. Finally ether with Al_2O_3 powder was used in order to get an undisturbed surface.

4. Results and discussion

4.1. XRD

An X-ray pattern of the sample with the nominal composition $Bi_{1.65}Pb_{0.35}Sr_2Ca_2Cu_3O_yF_{0.7}$ (Fig. 1(a)) shows the presence of mixed oxides and the 2 2 1 2 BSCCO phase already after preliminary calcination at 773 K. The only simple oxide registered in the sample was CuO. After the second heat treatment, at 1073 K for 3 h, the high T_c 2 2 2 3 phase appeared. A single phase 2 2 2 3 pattern was observed after 48 h sintering at 1113 K with one intermediate pulverizing and re-pelletizing (the lowest pattern in Fig. 1(a) with the peak assignment in accord with [23]). For comparison, in an undoped sample (Fig. 1(b)) simple oxides SrO and CaO were observed along with CuO even after the second heat treatment (1073 K), and traces of the 2 2 1 2 phase still remained in the sample after 120 h sintering at 1113 K. On the surface of the undoped pellet X-ray peaks at 18.99° and 39.33° characteristic of $Bi_2Sr_2O_5$ [24] were observed as well as the 5.78° reflection of the 2 2 1 2 compound [25]. Additional heat treatment of the fluorinated sample at 1113 K or increasing of the sintering temperature resulted in partial disintegration of the 2 2 2 3 phase. No significant shift of the X-ray peaks for the fluorine-substituted 2 2 2 3 was observed as compared to the undoped material (Fig. 1(a,b)) suggesting that the anionic radii of the oxide and fluoride ions are too close to influence noticeably the XRD pattern of this phase.

4.2. Atomic absorption

Atomic absorption spectroscopy of the sample with the XRD pattern shown in Fig. 1(a) gave the cation ratio Bi : Pb : Sr : Ca : Cu = 1.61 : 0.30 : 1.97 : 1.90 : 3.00. This is believed to correspond to the initial composition, within the experimental limits of the analytical method, estimated from the atomic absorption measurements of the blank with the same cation composition prepared by dissolving of the corresponding nitrates.
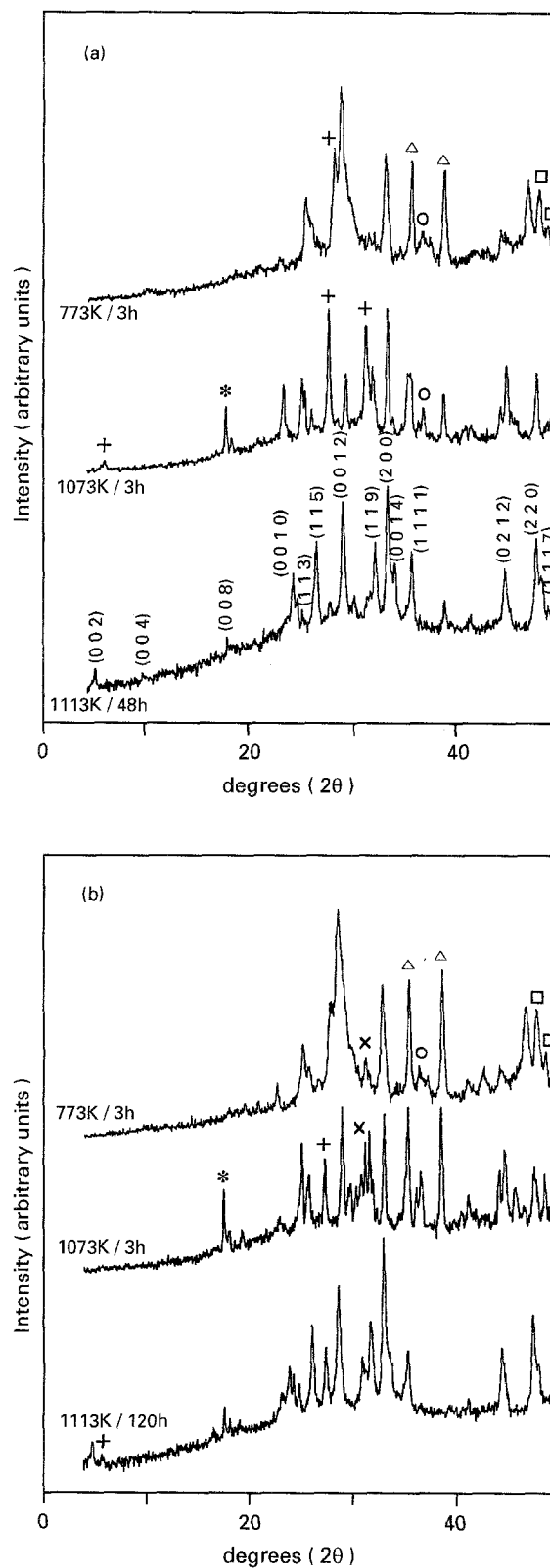

Figure 1 XRD patterns of BSCCO samples precalcined at 773 K and 1073 K and sintered at 1113 K. (a) with 0.7 at F/mol (nominal; (b) without fluorine. □ $Bi_2Sr_2CuO_6$; + 2 2 1 2; △ CuO; ○ Ca_2CuO_3; *Ca_2PbO_4; × (Sr,Ca) O.

4.3. Potentiometric determination of fluorine

Potentiometric determination of fluorine with the standard fluoride selective electrode showed that the sintered pellet contained only a fraction (up to 10%) of fluorine initially introduced (Table II). The main part of fluorine vaporized, presumably as HF, in the

TABLE II Fluoride concentrations (at F per formula) initially introduced and measured with the fluoride selective electrode

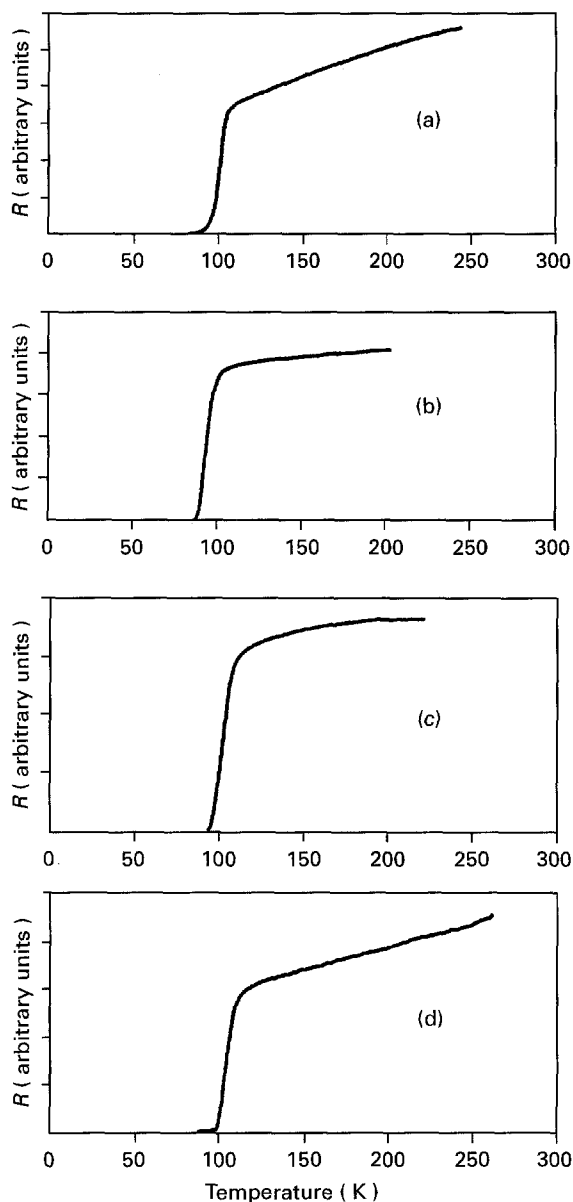| Sample #	[F] Introduced	[F] Measured
1	0.2	0.04
2	0.4	0.02
3[a]	0.7	0.18
4	0.7	0.07
5	2.0	0.07

[a] After precalcination at 1073 K/3 h.

Figure 2 R versus T curves for samples sintered at 1113 K. (a) 0.4 at F/mol BSCCO, sintered for 48 h; (b) 0.7 at F/mol, 72 h; (c) 0.7 at F/mol, 48 h; (d) without fluorine, 120 h.

Figure 3 Superconductivity transition in the sample shown in (Fig. 2, (c)) as measured by the inductive method.

preliminary stages of the preparation, prior to sintering of the pellet (sample #3 in Table II), since the cation composition of the sample remained essentially unchanged. This result corroborates the conclusion made on the basis of the analysis of the vapour composition presented in Table I: the partial pressure of HF at 1073 K is four to six orders of magnitude greater than that for metal fluorides. The analytical results in Table II are accurate to within 5% as
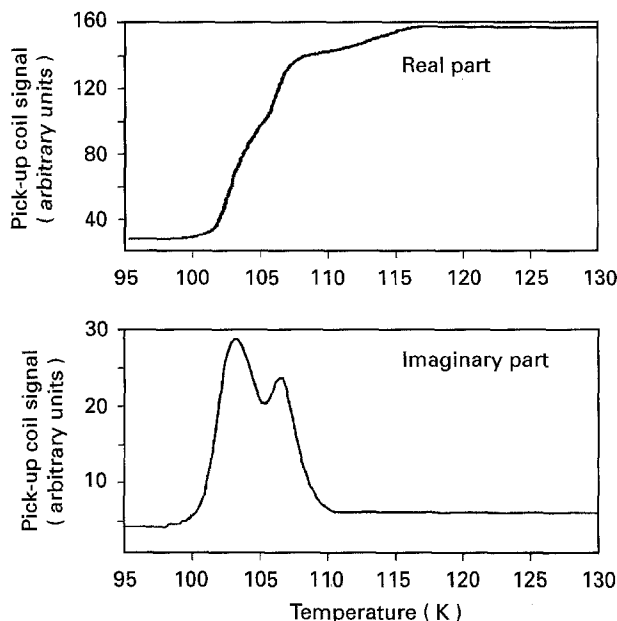
estimated from the measurements of the fluorine concentration in a number of blank mixtures of the corresponding nitrates and PbF_2 made against the same NaF standards.

4.4. Resistance

Fig. 2 shows the temperature dependences of the resistance for four samples with different fluorine concentrations and different heat treatments. Fig. 2(a) is for a sample with 0.4 fluorine atoms per formula (nominally), sintered at 1113 K for 192 h. The sample shown in Fig. 2(b) has a nominal fluorine content of 0.7 atoms per formula and was sintered at 1123 K for 72 h. The graph in Fig. 2(c) was obtained on a sample with 0.7 F at/mol sintered at 1113 K/48 h (the XRD pattern of this sample is shown in Fig. 1(a). An undoped 2 2 2 3 pellet sintered at 1113 K for as long as 120 h resulted in Fig. 2(d) (the corresponding XRD is shown in Fig. 1(b)). The highest T_c was observed for the sample shown in Fig. 2(c) with the shortest sintering time. It should be noted that the fluorine-free sample after the same heat treatment (1113 K/48 h) showed only a hint of superconducting transition above 77 K.

Superconducting transition for the pellet (Fig. 2(c)) was also traced by the inductive method [21] (Fig. 3). A similar two-peak pattern was observed on a sample without fluorine. In view of the high density of the shielding current induced in the samples as compared to that used normally in conventional four-point probe d.c. method [21], the two-peak pattern in Fig. 3 might have originated in two kinds of supercurrent loops with different j_c values, the first one corresponding to the sample as a whole and the second one to the intergrain areas [22]. Alternatively, the presence of two peaks may indicate that there are two states or phases in the sample with slightly different superconducting properties located in intergrain and boundary regions respectively.
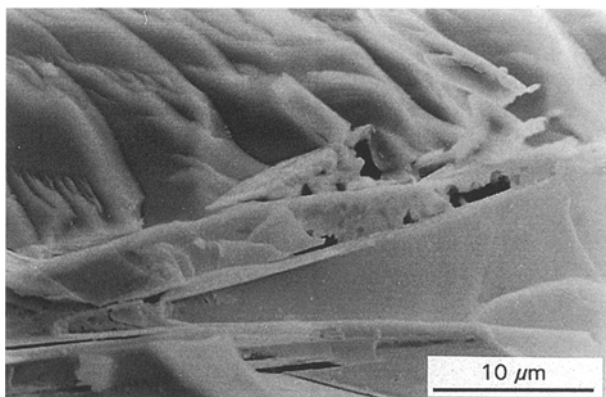
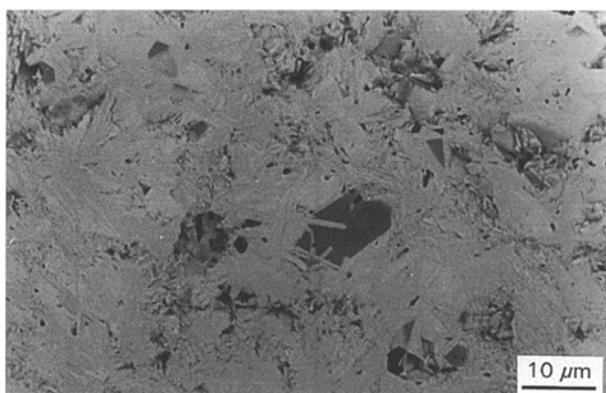*Figure 4* Secondary electron image (SEI) of the polished surface.

Figure 6 BEI of Ca_2CuO_3 prisms (dark) in the BSCCO matrix (bright) at the periphery of the pellet.

Figure 5 Backscatter electron image (BEI) of the polished pellet surface. Bright area is BSCCO, dark massive phase is (Sr,Ca)O.

Figure 7 X-ray distribution map of FK_α.

4.5. Electron probe microanalysis

Two samples were investigated by this method. The first observation of an unpolished surface of a pellet with an initial composition $Bi_{1.65}Pb_{0.35}Sr_2Ca_2Cu_3O_yF_{0.7}$, sintered at 1113 K for 48 h, gave an indication of the existence of traces of a Sr–Ca oxide phase along with the 2 2 2 3 BSCCO compound. Polishing of the surface with a water–ethanol-based mixture led to the disappearance of the Sr–Ca oxide phase; instead of this, etch pits were observed. Therefore, ether with Al_2O_3 powder was used subsequently. The morphology of the polished surface was examined by a secondary electron mode procedure (Fig. 4). Back scatter electron image (BEI) (Fig. 5) revealed the existence of two major phases: the "dark" one, with a lower mean atomic mass z, and the "light" phase, with a higher z. The analysis of the phases led to the following compositions: $Sr:Ca:Cu = 0.93:0.86:3.00$ for the (Sr, Ca)$_{14}Cu_{24}O_{41-x}$ (SCCO) phase and $Bi:Pb:Sr:Ca:Cu = 1.79:0.43:1.97:2.00:3.00$ for BSCCO phase. The BEI of BSCCO showed that the phase was not exactly uniform in composition as regards to the (Bi + Pb) content. Processing of BEI performed on several locations of the surface allowed the estimation of the ratio of the phases in the sample. On average there was 85–92% of BSCCO 2 2 2 3 phase while SCCO was 5–10%, the remaining area being porosity. Both untreated and polished surfaces were examined for the presence of fluorine. Unfortunately, no quantitative results could be obtained from these observations,
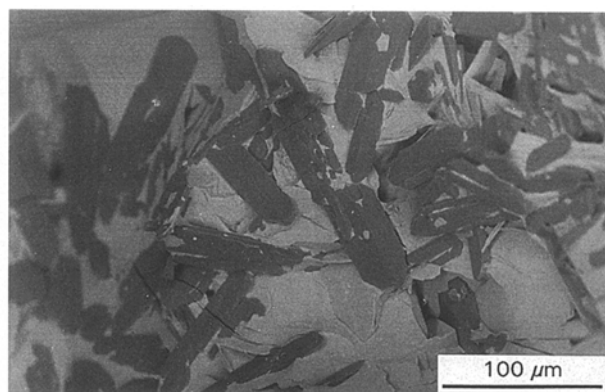
since the fluorine signal rapidly decreased in intensity, obviously meaning that fluorine vaporized under the beam.

Examination of the second sample (nominal composition $Bi_{1.8}Pb_{0.4}Sr_2Ca_2Cu_3O_yF_3$, sintered for 24 h at 1103 K) was made on an untreated surface. As a consequence, the quantitative results should be considered somewhat less accurate than those obtained on a polished surface. The inner part of the pellet was ingrown with extended prisms, a few mm long. The composition of these crystals corresponded to $(Sr, Ca)_{14}Cu_{24}O_y$. The pellet crust was defined as a mixture of 2 2 2 3 (major) and 2 2 1 2 (minor). Fig. 6 shows small crystals, identified as Ca_2CuO_3, in the BSCCO 2 2 2 3 matrix. Fig. 7 is a distribution map of fluorine on the pellet surface. The fluorine-containing phase is 2 2 1 2.

4.6. DTA/TGA

DTA traces of the 2 2 2 3 samples, both with and without fluorine, after the preliminary stage of preparation (precalcination at 773 K for 3 h), exhibited a small endothermic effect at 933 K and two pronounced peaks at higher temperatures, depending on the doping level. For pure 2 2 2 3 phase with $Bi:Pb = 1.8:0.4$ (Fig. 8(a)) the temperatures were 1038 K and 1093 K while for a sample with two fluorine atoms per mol (nominal composition) the corresponding temperatures were 1018 K and 1083 K
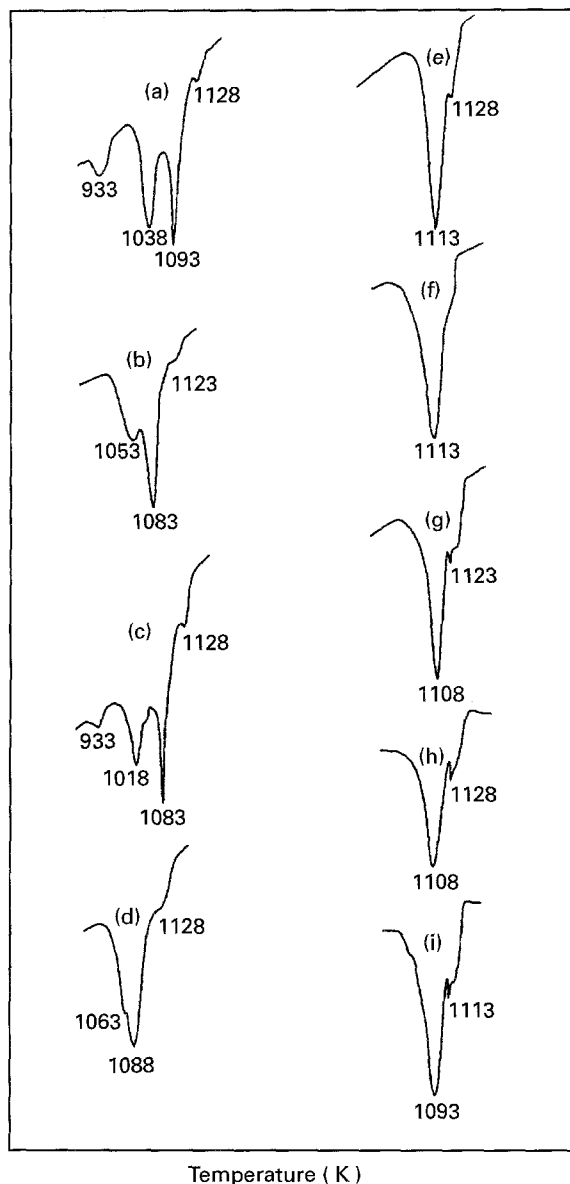
5107

Temperature (K)

Figure 8 DTA traces for precalcined 2 2 2 3 powders (a–d) and sintered pellets (e–i). (a) without fluorine, 773 K/3 h; (b) without fluorine, 1073 K/3 h; (c) 2.0 at F/mol BSCCO, 773 K/3 h; (d) 2.0 at F/mol, 1073 K/3 h; (e) 2 2 1 2; (f) 2 2 2 3 without fluorine, 1113 K/120 h; (g) 0.2 at F/mol, 1113 K/48 h; (h) 0.7 at F/mol, 1113 K/48 h; (i) 2.0 at F/mol, 1113 K/48 h.

(Fig. 8(c)). It can be seen in Fig. 8 that the shapes of these two peaks are quite different: the first one is broad while the second is sharp. An additional small peak at 1128 K was also observed for both samples. After the second stage treatment of the powder (1073 K, 3 h) the low temperature effect disappeared in both samples, leaving the DTA curve of the fluorinated sample with only one melting peak surrounded on both sides by shoulders (Fig. 8(d)). TGA curves showed considerable mass loss for both doped and undoped samples: about 12 mass % for 773 K/3 h samples and about 3–4 mass % for 1073 K/3 h samples. A 120 h heat treatment at 1113 K of the pellet with an intermediate pulverizing gave, for an undoped sample, a DTA scan with a single broad endothermic peak at 1113 K and a shoulder at a higher temperature (Fig. 8(f)). The shape of the peak is characteristic of the melting of a non-stoichiometric crystalline

phase. This melting temperature is suppressed when fluorine is introduced into the sample (Fig. 8(g–i)) implying that fluorine is partially substituted for oxygen. Also an additional small high-temperature effect is observed for the doped samples.

Thus, three endothermic peaks appeared in the DTA trace of the fluorine-free sample after precalcination of the sample at 773 K. The corresponding temperatures are 933, 1038 and 1093 K. No thermal effect was observed at 1003 K (solid state phase transition temperature in Bi_2O_3) meaning that pure Bi_2O_3 is not registered in the sample by DTA. This implies that mixed oxides are formed from a multicomponent mixture already at the preliminary stages of the process, even prior to calcination of the powder. Further proof of it is the endothermic peak at 933 K which, according to Majewski's [15] T–X phase diagram, corresponds to the formation of the 2 2 1 2 phase via the phase reaction

$$Bi_2Sr_2CuO_6 + 0.5\,Ca_2CuO_3$$
$$+ 0.5\,CuO \Rightarrow Bi_2Sr_2CaCu_2O_8 \qquad (1)$$
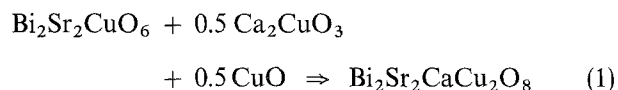
From the calorimetric data of Idemoto *et al.* [12] this reaction is indeed expected to be endothermic, with a small enthalpy change of $+ 22\,kJ\,mol^{-1}$ at 298 K. A broad endothermic peak at 1038 K for pure 2 2 2 3 (Fig. 8(a)) and at 1018 K for a doped sample (Fig. 8(c)) compares well with the high temperature limit of stability of $CaBi_2O_4$ reported by Roth and colleagues [26]; $CaBi_2O_4$ undergoes a peritectoid decomposition into Bi_2O_3-rich face-centred cubic solid solution and $Ca_2Bi_3O_{6.5}$ at 1051 K in air while in an inert atmosphere the phase transition temperatures in this system were proved to be 15 to 30 K lower [27]. The high temperature peak corresponds to the melting of the Pb-doped 2 2 1 2 phase formed in the phase reaction (Equation 1). Calcination of the material, both with and without fluorine, at 1073 K for 3 h resulted in the disappearance of the low temperature peak (Fig. 8(b,d)). Only the melting effect is registered with shoulders on both sides of it. Since a similar phase transformation route was observed in DTA traces of the 2 2 1 2 precalcined sample, it shows that the process shown in Equation 1 is essentially completed at the calcination stage of the synthesis.

A considerable mass loss of 12% is associated with elimination of the organics from the mixture, precalcined at 773 K. Calcination of the powder at 1073 K leads to complete removal of the organics and an additional mass loss of 3 to 4%. It does not originate in fluorine evolution since the mass loss is exactly the same for both pure and fluorine-doped samples.

DTA scan of the fluorine-free Bi(Pb) 2 2 2 3 pellet calcined for 120 h at 1113 K (Fig. 8(f)) exhibits a melting peak at 1113 K, in agreement with 1129 K for the melting of 2 2 2 3 without Pb [27] (it has been shown [28] that partial substitution of Pb for Bi in 2 2 2 3 led to decreasing of the phase transition temperatures). It took only 48 h for fluorinated samples, exposed to the same temperature treatment, to result in similar DTA scans, although the melting temperatures were somewhat lower, depending on fluorine

content (Fig. 8(g–i)). An additional small peak can be seen on these DTA traces which did not vanish even after repeated calcination of the pellets (72 h with intermediate pulverizing). It implies that the exact stoichiometry of the 2223 compound is outside the single-phase volume which is probably also true for the 2212 compound (Fig. 8(e)). Similar DTA curves were reported by Horiuchi and co-workers [9] for the fluorinated 2223 samples without Pb, prepared via solid state reaction, although these authors obtained only a multiphase sample.

5. Conclusion

An attempt has been made to partially substitute fluorine for oxygen in Bi(Pb) SCCO 2223 during the sol–gel citrate preparation of the material. Up to 10% of the nominal fluorine is introduced into the sample, while the rest of it evaporates as HF in the first stages of the preparation. The high-T_c phase is mainly formed at the sintering stages of the process via the phase reactions of the mixed oxides isolated from the mixture during the precalcination of the powder.

It has been shown that fluorine accelerated considerably the high-T_c phase formation in Bi–Pb–Sr–Ca–Cu–O; 48 h sintering of the F-doped sample at 1113 K resulted in XRD single phase 2223, while in a pure sample even after 120 h exposure traces of the 2212 phase were registered. Although no dramatic changes in zero resistance temperature of the material were detected, this procedure could be of significant interest for the preparation of thick films and tapes with no regrinding and much shorter heat treatment time as compared to both regular solid state reaction route, and even the sol–gel process without fluorine.

Acknowledgements

References

1. A. C. W. P. JAMES, S. M. ZAHURAK and D. W. MURPHY, *Nature* **338** (1989) 240.
2. A. TIGHEZZA, J. REHSPRINGER and M. DRILLON, *Physica C* **198** (1992) 209.
3. S. R. OVSHINSKY, R. T. YOUNG, D. D. ALLTRED, G. DEMAGGIO and G. A. VAN DER LEEDEN, *Phys. Rev. Lett.* **58** (1987) 2579.
4. H. H. WANG, A. M. KINI, H. I. KAO, E. H. APPELMAN, A. R. THOMPSON, R. E. BOTTO, K. D. CALSON, J. M. WILLIAMS and M. Y. CHEN, *Inorg. Chem.* **27** (1988) 5.
5. X. GAO, X. WU, H. YAN, Z. YIN, C. LIN, Y. FU and W. XIE, *Modern Phys. Lett.* **4** (1990) 137.
6. X. GAO, J. LI, D. GAO, G. ZHENG and S. GAO, *ibid.* **6** (1992) 943.
7. R. P. GUPTA, W. S. KHOKLE, J. C. PACHAURI, C. C. TRIPHATHI, B. C. PATHAK and G. S. VIRDI, *Appl. Phys. Lett.* **54** (1989) 570.
8. M. LEVINSON, S. S. P. SHAH and N. NAITO, *ibid.* **53** (1988) 922.
9. S. HORIUCHI, K. SKODA and Y. MATSEI, *J. Ceram. Soc. Jpn. Intern. Ed.* **97** (1989) 183.
10. W. QIN, Z. XIANGHUA, C. JIANGUO, G. XIAOHUI, W. XIAOLING and E. UINSEN, *Physica C* **208** (1993) 347.
11. E. KEMNITZ, S. SCHEURELL, S. W. NAUMOV, P. E. KASIN, V. I. PERSHIN and R. K. KREMER, *Eur. J. Sol. State Inorg. Chem.* **30** (1993) 701.
12. Y. IDEMOTO, K. SHIZUKA, V. YASUDA and K. FUEKI, *Physica C* **211** (1993) 36.
13. Y. IDEMOTO, K. SHIZUKA and K. FUEKI, *ibid.* **225** (1994) 127.
14. Thermodynamic Database Ivtantermo, Russian Academy of Science.
15. P. MAJEWSKI, *Adv. Mater.* (1994) in press.
16. G. B. SINYAREV, N. A. VATOLIN, B. G. TRUSOV and G. K. MOISEEV, "Application of computers for thermodynamic calculations of metallurgical processes" (Nauka Publishers, Moscow, 1982).
17. V. B. LAZAREV, K. S. GAVRICHEV and J. H. GREENBERG, *Pure & Appl. Chem.* **63** (1991) 1341.
18. L. BEN-DOR, H. DIAB and I. FELNER, *J. Sol. State. Chem.* **88** (1990) 183.
19. M. KAKIHANA, M. YOSHIMURA, H. MEZAKI, H. YASUOKA and L. BORJESSON, *J. Appl. Phys.* **71** (1992) 3904.
20. Y. K. SAN and W. Y. LEE, *Physica C* **212** (1993) 37.
21. J. H. CLAASEN, M. E. REEVES and R. J. SOULEN, *Rev. Sci. Instrum.* **62** (1991) 996.
22. V. E. KAZIN, T. E. OSKINA and Yu. D. TRETYAKOV, *J. Appl. Supercond.* **1** (1993) 1007.
23. S. M. GREEN, YU MEI, A. E. MANZI, H. L. LUO, R. RAMESH and G. THOMAS, *J. Appl. Phys.* **66/2** (1989) 728.
24. G. SPINOLO, U. ANSELMI-TAMBURINI, P. GHIGNA, G. CHIODELLI and G. FLOR, *J. Phys. Chem. Solids* **53** (1992) 591.
25. M. ONODA, A. YAMATO, E. TAKAYAMA-MUROMACHI and S. TAKEKAWA, *Jpn. J. Appl. Phys.* **27** (1988) L833.
26. R. S. ROTH, N. M. HWANG, C. J. RAWN, B. P. BURTON and J. J. RITTER, *J. Amer. Ceram. Soc.* **74** (1991) 2148.
27. M. R. De GUIRE, N. P. BANSAL, D. E. FARREL, V. FINAN, C. J. KIM, R. J. HILLS and C. J. ALLEN, *Physica C* **179** (1991) 333.
28. P. STROBEL, J. C. TOLEDANO, D. MORIN, J. SCHNECK, G. VACQUIER, O. MONNEREAU, J. PRIMOT and T. FOURNIER, *ibid.* **201** (1992) 27.